9098 Vol. 56, No. 32 / November 10 2017 / Applied Optics Research Article

applied optics

Positive dwell time algorithm with minimum equal extra material removal in deterministic optical surfacing technology

LONGXIANG LI,[1,2,*] DONGLIN XUE,[1,2] WEIJIE DENG,[1,2] XU WANG,[1,2] YANG BAI,[1,2] FENG ZHANG,[1,2] AND XUEJUN ZHANG[1,2]

[1]Key Laboratory of Optical System Advanced Manufacturing Technology, Chinese Academy of Sciences, Changchun 130033, China
[2]Changchun Institute of Optics, Fine Mechanics and Physics, Chinese Academy of Sciences, Changchun, Jilin 130033, China
*Corresponding author: leellxhit@126.com

Received 5 July 2017; revised 15 October 2017; accepted 16 October 2017; posted 16 October 2017 (Doc. ID 301538); published 9 November 2017

In deterministic computer-controlled optical surfacing, accurate dwell time execution by computer numeric control machines is crucial in guaranteeing a high-convergence ratio for the optical surface error. It is necessary to consider the machine dynamics limitations in the numerical dwell time algorithms. In this paper, these constraints on dwell time distribution are analyzed, and a model of the equal extra material removal is established. A positive dwell time algorithm with minimum equal extra material removal is developed. Results of simulations based on deterministic magnetorheological finishing demonstrate the necessity of considering machine dynamics performance and illustrate the validity of the proposed algorithm. Indeed, the algorithm effectively facilitates the determinacy of sub-aperture optical surfacing processes.

OCIS codes: (120.4610) Optical fabrication; (240.5450) Polishing; (240.0240) Optics at surfaces; (220.1250) Aspherics.

https://doi.org/10.1364/AO.56.009098

1. INTRODUCTION

In modern optical surfacing technologies, deterministic sub-aperture polishing and figuring techniques, including typically magnetorheological finishing (MRF) [1–3], ion beam figuring (IBF) [4,5], and so forth, have played a significant role in manufacturing high-precision mirrors. Based on a highly stable removal function (or influence function), realizing the dwell time accurately is one of the crucial factors guaranteeing a high-convergence ratio for the optical surface error. Therefore, the limitations of machine dynamics on the implementation of the theoretical dwell time cannot be ignored in reality.

Generally speaking, the dwell time algorithm in sub-aperture optical manufacturing technologies is based on the principle that the desired removal amounts of material in optics are discrete 2D convolution operations of the dwell time map and the removal function. With the development of sub-aperture optical manufacturing technologies, two main kinds of dwell time algorithms have been established. One is to deal with the discrete convolution model directly, such as in the Fourier transform method [6], the iterative method, and the series expansion method [7,8]. The other is to transform the convolution format into linear matrix equations in algebra and then to solve the linear matrix equations to obtain the dwell time distribution [9,10]. In the algorithms mentioned above, almost all the constraints on the dwell time map are non-negative, which means that the minimum value of the dwell time is zero. In fact, when a dwell time map is transformed into a dwell velocity map, the computer numeric control (CNC) system in a polishing machine cannot accurately execute high velocities beyond its dynamic capability. Song *et al.* [11] and Zhang *et al.* [12] added positive constraints on the dwell time based on linear matrix equations considering machine dynamics. However, accuracy of the optical surface shape could be further improved if the extra material removal had been considered. Wu *et al.* [13] pointed out that extra material removal is necessary in the dwell time algorithm, but they utilized a non-negative constraint without considering machine dynamics, and Wu *et al.* did not show any way of choosing a reasonable value for the extra material removal. In reality, much larger extra material removal may lead to an increased processing time in a deterministic finishing process, especially for large-aperture optics, while a smaller removal amount may lead to a decrease in the accuracy of the residual optical surface error. Therefore, to improve the determinacy and convergence efficiency of sub-aperture optical manufacturing technologies, the machine dynamics, residual surface error accuracy, and total polishing time must be taken into account simultaneously in the dwell time algorithm. In this paper, based on a non-negative approach, a high-precision dwell time algorithm under positive constraints is established with minimum equal extra material removal.

First, the non-negative dwell time algorithm based on the linear matrix equation is reviewed. Then, positive constraints on the solution domain of the dwell time are analyzed. A positive dwell time algorithm is established based on minimum equal extra material removal, which is studied in detail. Finally, the results of simulations prove the validity of the model and theory in this paper.

2. NON-NEGATIVE DWELL TIME ALGORITHM

A. Dwell Time Matrix Equation

The deterministic sub-aperture polishing techniques are typical kinds of computer controlled optical surfacing (CCOS). Generally, the process used to obtain the dwell time is a discrete 2D de-convolution in algebra [14], as shown in Eq. (1):

$$E(x_i, y_i) = \sum_{j=1}^{N} R(x_i - \xi_j, y_i - \eta_j) \cdot T(\xi_j, \eta_j). \tag{1}$$

Here $E(x_i, y_i)$ means the total removal amount at some point (x_i, y_i). $T(\xi_i, \eta_i)$ is the specific period of dwell time at the dwell point (ξ_i, η_i). $R(x_i - \xi_i, y_i - \eta_i)$ is related to the removal function, which means the material removal amount at data point (x_i, y_i) on the surface error map when the polishing tool dwells at the point (ξ_i, η_i). N is the total number of dwell points. Considering the process in which the polishing tool scans over the optical surface, a matrix product in algebra, instead of the convolution, can be obtained as shown in Eq. (2):

$$Rt = e. \tag{2}$$

In Eq. (2),

$$e = \begin{bmatrix} e_1 \\ e_2 \\ \vdots \\ e_M \end{bmatrix}, \quad t = \begin{bmatrix} t_1 \\ t_2 \\ \vdots \\ t_N \end{bmatrix}, \quad R = \begin{bmatrix} r_{11} & r_{12} & \cdots & r_{1N} \\ r_{21} & r_{22} & \cdots & r_{2N} \\ \vdots & \vdots & \ddots & \vdots \\ r_{M1} & r_{M2} & \cdots & r_{MN} \end{bmatrix}. \tag{3}$$

R is called the removal function matrix, e is the initial surface error map on the optical surface, and t is the period of dwell time distributed at different dwell points. The dwell time t can be gained by solving Eq. (2), which is a typical inverse problem in mathematics. M is the total number of data points from a discrete optical surface error map.

B. Non-Negative Dwell Time Solution

In Ref. [15], we emphasized that a non-negative constraint has to be attached to the dwell time in Eq. (2), which can be described as

$$Rt = e, \qquad t \geq 0. \tag{4}$$

According to Eq. (4), the process to obtain the dwell time is a non-negative least-squares (NNLS) problem in mathematics. Considering the Tikhonov regulation parameter β needed to maintain the stability of the solution, the optimized format of the dwell time NNLS problem is presented as follows:

$$\underset{t}{\text{minimize}}\, f(t) = [\|Rt - e\|^2 + \beta \|It\|^2], \qquad t \geq 0. \tag{5}$$

With the help of Eq. (3), Eq. (5) can also be expressed as

$$\underset{t}{\text{minimize}}\, f(t) = \sqrt{\sum_{j=1}^{N}\left[\sum_{i=1}^{M}(r_{ij}t_j - e_i)^2\right] + \beta^2 \sum_{j=1}^{N} t_j^2}, \qquad t \geq 0. \tag{6}$$

The combination of the constrained generalized minimal residual method (CGMRES) and adaptive Tikhonov regulation is a good choice to solve Eq. (6) with a high accuracy and calculation efficiency [15]. The final dwell time distribution solved by the non-negative algorithm in Ref. [15] is denoted as $T_{\text{non-neg}}$. By considering Eq. (1), the residual surface error at the data point (x_i, y_i) is $\gamma(x_i, y_i)$, as shown in Eq. (7):

$$\gamma(x_i, y_i) = \sum_{j=1}^{N} R(x_i - \xi_j, y_i - \eta_j) \cdot T_{\text{non-neg}}(\xi_j, \eta_j) - E(x_i, y_i). \tag{7}$$

A reasonable non-negative solution makes $\gamma(x_i, y_i)$ tend to zero. The distribution of the residual surface error is $\gamma(x, y)$.

3. POSITIVE CONSTRAINTS ON DWELL TIME

In deterministic sub-aperture polishing processes, the dwell time is usually transferred to velocity instructions to control the tool when moving from one dwell point to another along a planned path, which is usually called the velocity control model, Ref. [16]. When the polishing tool characterized by its removal function moves from dwell point a to points b, c, and d, as shown in Fig. 1(a), some types of velocity control

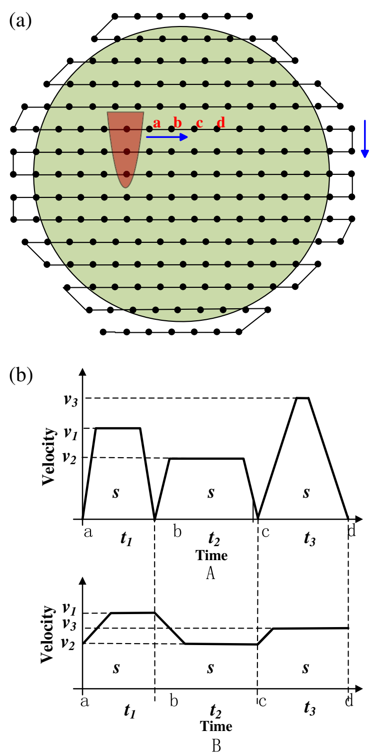

Fig. 1. MRF polishing tool, characterized by its removal function, scans on an optical surface along a raster path. (a) Scanning path from one dwell point to another. (b) Some examples of velocity control models.

models in MRF are proposed, for instance, as shown in Fig. 1(b). In Fig. 1(b), t is the period of dwell time, and s is the step size of the dwell points along the path. Model A describes a polishing tool, the velocity of which decreases to zero each time before it moves to the next point. In contrast, in model B, the CNC system controls the velocity of the polishing tool so that it does not have to be zero when it moves from one point to another. Obviously, for any model, the performance of the maximal velocity and acceleration of the machine must be considered.

However, considering the above discussion, a non-negative constraint in the dwell time like that in Eq. (4) is not accurate enough for a deterministic sub-aperture polishing process, as the limitations of the machine kinematic performance are not taken into account. In other words, when the dwell time is zero or near zero at some dwell points on optical surfaces, the corresponding velocity and acceleration of the moving axes in the CNC machine approach infinite values, which is impossible in practice. Therefore, more rigorous constraints than in Eq. (4) must be attached to the dwell time in Eq. (2), which is described as follows:

$$Rt = e, \quad \begin{cases} \sigma \le t \\ 0 < \sigma \end{cases}. \tag{8}$$

In Eq. (8), σ is the minimum period of the dwell time between two adjacent dwell points considering the performance of the maximum velocity and acceleration of CNC machines according to specific velocity control models. With the help of the regularization parameter β, the optimized goal of Eq. (8) as a constrained least-squares problem is shown in Eq. (9), replacing Eq. (6):

$$\underset{t}{\text{minimize}}\, f(t) = \sqrt{\sum_{j=1}^{N}\left[\sum_{i=1}^{M}(r_{ij}t_j - e_i)^2\right] + \beta^2\sum_{j=1}^{N}t_j^2}, \quad \begin{cases} \sigma \le t \\ 0 < \sigma \end{cases}. \tag{9}$$

4. POSITIVE DWELL TIME ALGORITHM

A. Minimum Equal Extra Material Removal

From the view point of algebra, those rigorous constraints on the dwell time in Eq. (8) lead to a reduction of the dwell time solution's freedom. A progressive algorithm must be discussed. First, the minimum extra material removal, which ensures a good balance between the total polishing time and the accuracy of the residual surface error, is introduced in this section.

The dwell time map with positive constraints as in Eq. (8) is noted as T_p. By considering an extra material removal $h(x_i, y_i)$, a modified equation based on Eq. (1) is described as in Eq. (10):

$$E(x_i, y_i) + h(x_i, y_i) = \sum_{j=1}^{N} R(x_i - \xi_j, y_i - \eta_j) \cdot T_p, \tag{10}$$

where $h(x_i, y_i)$ means that the extra material removal is related to the positions of the polishing tool on the optical surface.

Considering $T_{\text{non-neg}}$, which is the dwell time map with non-negative constraints mentioned above, T_p can be set as follows:

$$T_p = T_{\text{non-neg}} + \sigma. \tag{11}$$

Obviously, this T_p meets the positive constraint conditions from the machine dynamics, and Eq. (10) can be transformed as follows:

$$E(x_i, y_i) + h(x_i, y_i) = \sum_{j=1}^{N} R(x_i - \xi_j, y_i - \eta_j) \cdot T_{\text{non-neg}}(\xi_j, \eta_j) + \sigma \sum_{j=1}^{N} R(x_i - \xi_j, y_i - \eta_j). \tag{12}$$

Equation (12) can also be expressed as Eq. (13):

$$\sum_{j=1}^{N} R(x_i - \xi_j, y_i - \eta_j) \cdot T_{\text{non-neg}}(\xi_j, \eta_j) - E(x_i, y_i) = h(x_i, y_i) - \sigma \sum_{j=1}^{N} R(x_i - \xi_j, y_i - \eta_j). \tag{13}$$

Apparently, the left side of Eq. (13) represents the residual surface error at data point (x_i, y_i) by the non-negative constraint dwell time solution and is noted as $\gamma(x_i, y_i)$:

$$\gamma(x_i, y_i) = \sum_{j=1}^{N} R(x_i - \xi_j, y_i - \eta_j) \cdot T_{\text{non-neg}}(\xi_j, \eta_j) - E(x_i, y_i) = h(x_i, y_i) - \sigma \sum_{j=1}^{N} R(x_i - \xi_j, y_i - \eta_j). \tag{14}$$

As mentioned in Section 2, the theoretically ideal value of $\gamma(x_i, y_i)$ is zero. Therefore, a minimum extra material removal $h_m(x_i, y_i)$ at data point (x_i, y_i) is obtained, as shown in Eq. (15). The minimum extra material removal distribution at any data point is expressed as $h_m(x, y)$:

$$h_m(x_i, y_i) = \sigma \sum_{j=1}^{N} R(x_i - \xi_j, y_i - \eta_j). \tag{15}$$

In Eq. (15), σ is the positive dwell time constraint. $R(x_i - \xi_i, y_i - \eta_i)$ is related to the removal function (influence function), the data points (x_i, y_i) on the initial surface error profile, and the dwell points (ξ_i, η_i) on the tool path. Once the positive dwell time constraint, the removal function, the data points, and the dwell points are chosen, the minimum extra material removal $h_m(x_i, y_i)$ can be calculated according to Eq. (15). An IBF and an MRF removal function are taken as examples to calculate the extra material removal $h_m(x_i, y_i)$, as shown in Fig. 2, ignoring the edges. Figure 2(a) and Fig. 2(c) show the removal function of MRF and IBF, respectively. Figure 2(b) and Fig. 2(d) show the minimum extra material removal $h_m(x_i, y_i)$ for MRF and IBF, respectively.

In practice, an equal extra material removal is essential to obtain a theoretically ideal optical surface. Considering the peak-to-valley (PV) of the extra material removal distribution, the minimum value of the equal extra material removal, defined as h_0, is described in Eq. (16) and graphically illustrated in Fig. 3:

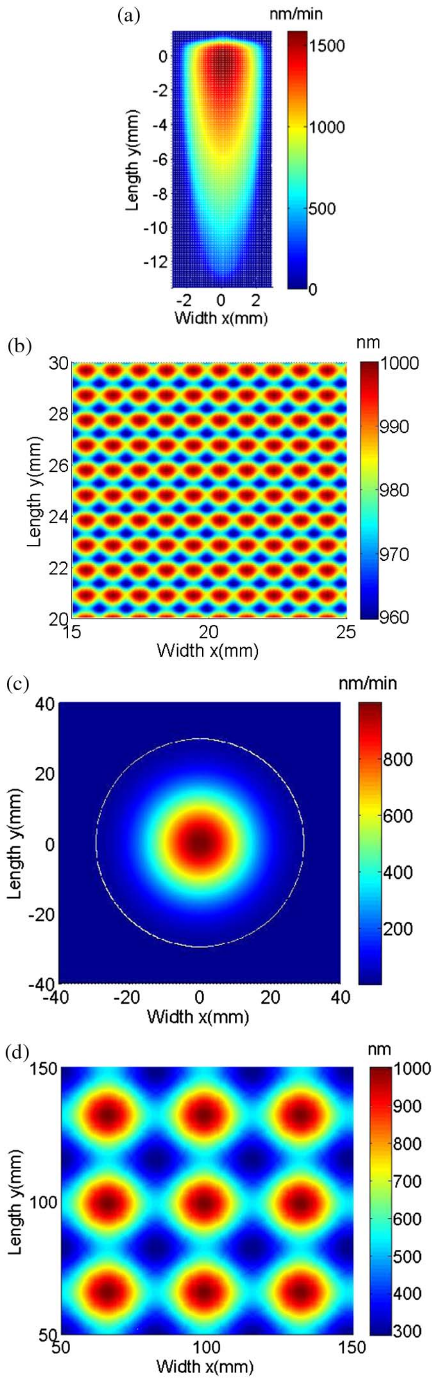

Fig. 2. Distribution of extra material removal. (a) MRF removal function. (b) MRF 2D extra material removal. (c) IBF removal function. (d) IBF 2D extra material removal.

$$h_0 = \max\{h_m(x_i, y_i)\}. \quad \textbf{(16)}$$

Apparently, the minimum equal extra material removal h_0 is a uniform material layer and related to the positive dwell time constraint σ, the removal function, the parameters of the data points on the initial surface error profile, and the parameters of the dwell points on the polishing path. By Eqs. (15) and (16), a proper value of the uniform material layer is obtained. Then,

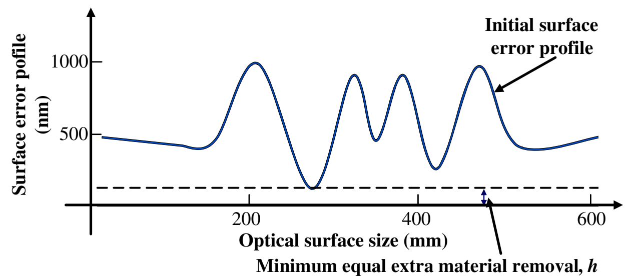

Fig. 3. Equal extra material removal.

the minimum equal extra material removal h_0 is added to the initial surface error profile to calculate the dwell time map.

B. Dwell Time Algorithm with Positive Constraints

When h_0, the minimum equal thickness of the extra material removal, is added to the initial surface error map, the optimized goal of the solving process for dwell time is expressed in another format, shown in Eq. (17), compared with Eq. (9):

$$\underset{t}{\text{minimize}}\, f(t) = \sqrt{\sum_{j=1}^{N}\left[\sum_{i=1}^{M}(r_{ij}t_j - e_i - h_0)^2\right] + \beta^2 \sum_{j=1}^{N} t_j^2}, \quad \begin{cases} \sigma \le t \\ 0 < \sigma \end{cases}. \quad \textbf{(17)}$$

Based on the non-negative constraint dwell time map $T_{\text{non-neg}}$, the solution of Eq. (17) is set as T_p, as shown in Eq. (11). The residual surface error distribution $\varepsilon(x, y)$ of the positive constraint algorithm is analyzed as follows. Considering some specific data point (x_i, y_i), the residual surface error $\varepsilon(x_i, y_i)$ is expressed as Eq. (18) with the help of Eq. (19):

$$\begin{aligned}\varepsilon(x_i, y_i) &= [E(x_i, y_i) + h_0] \\ &\quad - \left[\sum_{j=1}^{N} R(x_i - \xi_j, y_i - \eta_j) \cdot T_{\text{non-neg}}(\xi_j, \eta_j) + \sigma \sum_{j=1}^{N} R(x_i - \xi_j, y_i - \eta_j)\right] \\ &= \Delta h(x_i, y_i) - \gamma(x_i, y_i),\end{aligned} \quad \textbf{(18)}$$

$$\Delta h(x_i, y_i) = h_0 - h_m(x_i, y_i). \quad \textbf{(19)}$$

The residual surface error $\varepsilon(x_i, y_i)$ is comprised of two minimal items: $\gamma(x_i, y_i)$ is the residual surface error map with non-negative constraints, and $\Delta h(x_i, y_i)$ is related to the removal rate distribution of the removal function and the tool path parameters.

Indeed, $\Delta h(x_i, y_i)$ has an explicit physical meaning that reflects the tool path ripple [17] caused by the equal extra material removal. The dwell time algorithm obtains a simulated residual surface error map based on the rule that the polishing tool remains at every discrete dwell point on the tool path. In contrast, in the velocity control models mentioned above, the polishing tool moves continuously with different velocities between the adjacent dwell points, as shown in Fig. 1(b). In this situation, although $\Delta h(x_i, y_i)$ cannot exactly represent the distribution of the tool path ripple in the continuous velocity control model, its value indeed reflects the extent of the real tool path ripple caused by the equal extra material removal in deterministic polishing techniques.

According to Eq. (18), if the equal extra material removal is determined and the removal function and the tool path parameters are chosen definitively, the residual surface error $\varepsilon(x, y)$ is affected only by the non-negative constraint residual surface error of $\gamma(x, y)$. That is, in this situation, the accuracy and calculation efficiency of the dwell time algorithm with positive constraints is determined only by the non-negative dwell time algorithm, as shown in Eq. (11). Moreover, not only the algorithm mentioned in Section 2 but also any other non-negative dwell time algorithm can be applied to Eq. (11) to obtain T_p with positive constraints.

5. SIMULATIONS

In order to prove the validity of the dwell time algorithm under a positive constraint with the minimum equal extra material removal, simulations were conducted based on deterministic surface techniques. In this paper, MRF is taken as an example.

A. Necessity of Positive Constraints on the Dwell Time

When a non-negative dwell time map is transformed into a distribution of velocities, those values within the constraints of the performance of the machine's velocity and acceleration can be executed; otherwise, high or infinite values cannot be executed exactly in the real polishing process. As a result, the residual surface errors in some local areas are converged effectively, and those in other local areas are not. A simulation was conducted to demonstrate this phenomenon.

The initial surface error map was chosen as shown in Fig. 4(a), and the applied MRF removal function is given in Fig. 2(a). The distances between the adjacent data points on the surface error map and the value between the adjacent dwell points along the raster tool path are both 1 mm. First, the non-negative dwell time map and the corresponding virtual simulated residual error map were obtained, as shown in Figs. 4(b) and 4(c), by the non-negative algorithm we have published in Ref. [15]. The PV and root mean square (RMS) value of the residual error map are 28.04 nm and 1.50 nm, respectively. In the dwell time map, the minimum value of the dwell time is zero and the total polishing time is 0.32 h. Then, considering that the constraints of the machine dynamics lead to a minimum dwell time value σ, in the non-negative dwell time map, values less than σ are set to σ, and others are kept the same as the original. This way of changing the non-negative dwell time map simulates the real process by which the CNC machine executes the velocities transformed from the dwell time. Sigma was set to 50 ms and 100 ms to show the machine dynamics' effects on the residual error in reality. As shown in Figs. 4(d)–4(g), with the increase of σ, the values of the PV and RMS of the residual error become greater, which means that the worse the performance of the machine dynamics, the lower the accuracy of the optic's surface shape after figuring by utilization of the non-negative dwell time map. Therefore, the non-negative constraint on the dwell time algorithm alone cannot guarantee the determinacy of optical surfacing techniques such as MRF and IBF. Positive constraints are necessary for an effective dwell time algorithm.

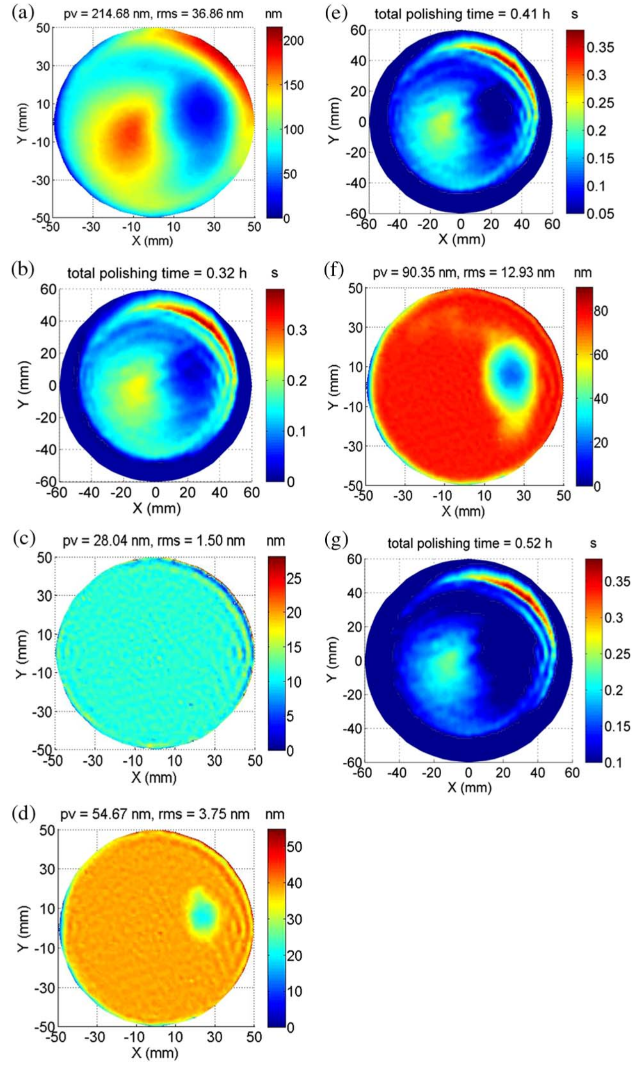

Fig. 4. Real residual surface error based on non-negative dwell time map. (a) Initial surface error map. (b) Dwell time map with $\sigma = 0$ ms. (c) Residual error map with $\sigma = 0$ ms. (d) Residual error map with $\sigma = 50$ ms. (e) Dwell time map with $\sigma = 50$ ms. (f) Residual error map with $\sigma = 100$ ms. (g) Dwell time map with $\sigma = 100$ ms.

B. Positive Dwell Time Algorithm with Minimum Equal Extra Material Removal

In order to prove the validity of the positive dwell time map and the minimum equal extra material removal, as shown in Eq. (11) and Eq. (16), respectively, a simulation was conducted based on the same parameters mentioned in Section 5.A, including initial surface error map and removal function. The non-negative dwell time map $T_{\text{non-neg}}$ is calculated as shown in Fig. 4(c). The σ constrained by the machine dynamics is supposed to be 50 ms. Hence, the minimum equal extra material removal h_0 is 41.05 nm, and the positive dwell time T_p shown in Fig. 5(b) differs from that displayed in Fig. 4(e). Additionally, the total value of T_p (polishing time) is obviously

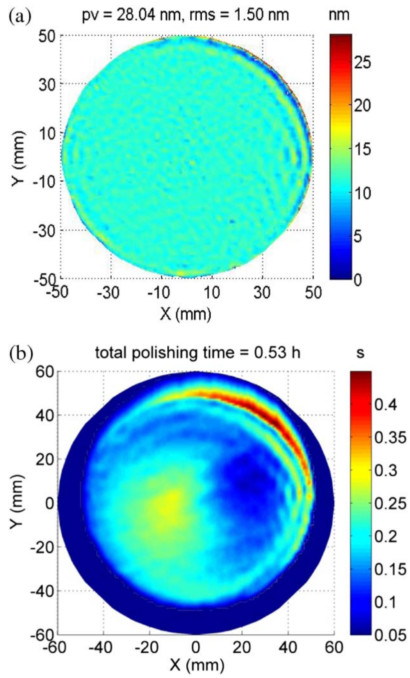

Fig. 5. Simulation results of the positive dwell time algorithm. (a) Residual error map with $\sigma = 50$ ms. (b) Dwell time map with $\sigma = 50$ ms.

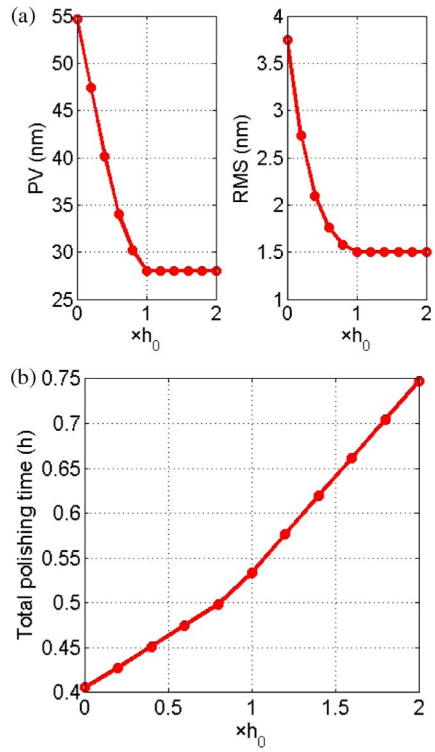

Fig. 6. PV, RMS, and polishing time for different multiples of the equal extra material removal value h_0. (a) Value of the PV and RMS. (b) Total polishing time.

greater than that of $T_{\text{non-neg}}$. Moreover, on one hand, because the step sizes of data points and dwell points are both 1 mm, in the discrete numerical simulation, the residual error $\Delta h(x_i, y_i)$ is zero in Eq. (18). The residual surface error from the positive dwell time algorithm is simply equal to $\gamma(x_i, y_i)$. On the other hand, in the simulation, the corresponding residual surface error described in Fig. 5(a) is exactly the same as in Fig. 4(c). The high accuracy and consistency of the residual surface error profile from the positive and non-negative dwell time algorithm proved that the algorithm proposed in this paper is effective and valid in deterministic polishing and figuring techniques.

Moreover, the minimum equal extra material removal's validity is proved in the following numerical simulation. As calculated above, while σ is 50 ms, the minimum equal extra material removal h_0 is 41.05 nm. The different values of the equal extra material removal are set. When the value of the equal extra material removal is less than h_0, the corresponding minimum value of the dwell time is less than 50 ms, and these dwell time periods cannot be executed accurately. As a result, the PV and RMS values of the residual surface error in reality, as shown in Fig. 6(a), are greater than those values given in Fig. 5(a). In contrast, when the value of the equal extra material removal is greater than h_0, the minimum value of the dwell time is greater than 50 ms, and all the dwell times can be executed accurately by the CNC machine. Consequently, the PV and RMS values of the residual surface error in reality, as shown in Fig. 6(a), are kept the same as those in Fig. 5(a). Therefore, the h_0 is proved to be the minimum equal extra material removal in numerical simulation. Finally, it cannot be ignored that the total dwell time becomes longer with increased equal extra material removal, as shown in Fig. 6(b), which is consistent with the real optical figuring process.

6. CONCLUSIONS

Considering the execution accuracy of the dwell time by a CNC system in reality, positive constraints were added to the dwell time solution in sub-aperture optical surfacing techniques. The limitations of machine dynamics on the dwell time distribution were analyzed, and a strategy for obtaining the minimum equal extra material removal was devised. A positive dwell time algorithm was established based on a non-negative algorithm with the help of extra material removal. The necessary minimum equal extra material removal can be calculated to balance the total polishing time and the accuracy of the residual surface error profile according to this paper.

Further simulations indicate that limitations of the machine dynamics decrease the determinacy of the sub-aperture optical surfacing techniques based on the non-negative dwell time algorithm. Positive constraints are necessary for a reasonable dwell time algorithm in reality. Moreover, in the simulation example the positive dwell time algorithm converges the PV from 214.678 to 28.04 nm and the RMS from 26.86 to 1.50 nm, with 41.05 nm minimum equal extra material removal, considering the 50 ms dwell time constraint from the machine dynamics. This indicates that the positive dwell time algorithm with minimum equal extra material removal is valid and effective. Generally, the model and algorithm developed in this paper could be widely applied for other computer control optical surfacing processes.

Funding. National Natural Science Foundation of China (NSFC) (61605202); Chinese Academy of Sciences Key Project (CAS Key Project) (QYZDJ-SSW-JSC038-02).

REFERENCES

1. A. Sidpara, "Magnetorheological finishing: a perfect solution to nanofinishing requirements," Opt. Eng. **53**, 092002 (2014).
2. S. Salzman, H. J. Romanofsky, G. West, K. L. Marshall, S. D. Jacobs, and J. C. Lambropoulos, "Acidic magnetorheological finishing of infrared polycrystalline materials," Appl. Opt. **55**, 8448–8456 (2016).
3. M. Beier, S. Scheiding, A. Gebhardt, R. Loose, S. Risse, R. Eberhardt, and A. Tünnermann, "Fabrication of high precision metallic freeform mirrors with magnetorheological finishing (MRF)," Proc. SPIE **8884**, 88840S (2013).
4. M. Civitani, M. Ghigo, J. Hołyszko, G. Vecchi, and S. Basso, "Ion beam figuring of thin glass plates: achievements and perspectives," Proc. SPIE **9905**, 990578 (2016).
5. T. Arnold and F. Pietag, "Ion beam figuring machine for ultra-precision silicon spheres correction," Precis. Eng. **41**, 119–125 (2015).
6. S. R. Wilson and J. R. McNeil, "Neutral ion beam figuring oflarge optical surfaces," Proc. SPIE **818**, 320–324 (1987).
7. T. W. Drueding, T. G. Bifano, and S. C. Fawcett, "Contouring algorithm for ion figuring," Precis. Eng. **17**, 10–21 (1995).
8. G. Sandri, M. N. Horenstein, M. R. Feinberg, P. M. Shanbhag, and T. G. Bifano, "Ion-beam machining of millimeter scale optics," Appl. Opt. **39**, 599–611 (2000).
9. S. Wilson and J. McNeil, "Neutral ion beam figuring of large optical surfaces," Proc. SPIE **0818**, 320–324 (1987).
10. W. Deng, L. Zheng, Y. Shi, X. Wang, and X. Zhang, "Dwell time algorithm based on matrix algebra and regularization method," Opt. Precis. Eng. **15**, 1009–1015 (2007) [in Chinese].
11. C. Song, Y. Dai, and X. Peng, "Model and algorithm based on accurate realization of dwell time in magnetorheological finishing," Appl. Opt. **49**, 3676–3683 (2010).
12. Y. Zhang, Y. Wang, Y. J. Wang, J. He, and W. Huang, "Dwell time algorithm based on the optimization theory for magnetorheological finishing," Proc. SPIE **7655**, 76551V (2010).
13. J. Wu, Z. Lu, H. Zhang, and T. Wang, "Dwell time algorithm in ion beam figuring," Appl. Opt. **48**, 3930–3937 (2009).
14. R. A. Jones, "Optimization of computer controlled polishing," Appl. Opt. **16**, 218–224 (1977).
15. L. Li, L. Zheng, W. Deng, X. Wang, X. Wang, B. Zhang, Y. Bai, H. Hu, and X. Zhang, "Optimized dwell time algorithm in magnetorheological finishing," Int. J. Adv. Manuf. Technol. **81**, 833–841 (2015).
16. C. Jiao, "Study on the material removal mechanisms and fundamental processes for ion beam figuring optical mirrors," Ph.D. dissertation (National University of Defense Technology, 2008) [in Chinese].
17. H. Hu, Y. Dai, and X. Peng, "Restraint of tool path ripple based on surface error distribution and process parameters in deterministic finishing," Opt. Express **18**, 22973–22981 (2010).